Exp. Anim. 63(2), 215–225, 2014

—Original—

Transcriptional and Histological Analyses of the Thymic Developmental Process in the Fetal Pig

Shunichi SUZUKI[1)], Misae SUZUKI[1)], Michiko NAKAI[1)], Shoichiro SEMBON[1)], Daiichiro FUCHIMOTO[1)], and Akira ONISHI[1)]

[1)]*Transgenic Pig Research Unit, National Institute of Agrobiological Sciences, 2 Ikenodai, Tsukuba, Ibaraki 305-0901, Japan*

Abstract: The humanized pig model, in which human cells or tissues can be functionally maintained in pigs, can be an invaluable tool for human medical research. Although the recent development of immunodeficient pigs has opened the door for the development of such a model, the efficient engraftment and differentiation of human cells may be difficult to achieve. The transplantation of human cells into fetal pigs, whose immune system is immature, will ameliorate this problem. Therefore, we examined the development of porcine fetal thymus, which is critical for the establishment of the immune system. We first analyzed the levels of mRNA expression of genes that are relevant to the function of thymic epithelial cells or thymocytes in whole thymi from 35 to 85 days of gestation (DG) and at 2 days postpartum (DP) by quantitative RT-PCR. In addition, immunohistochemical analyses of thymic epithelial cells from DG35 to DG55 and DP2 were performed. These analyses showed that the thymic cortex was formed as early as DG35, and thymic medulla gradually developed from DG45 to DG55. These findings suggested that, at least before DG45, the thymus do not differentiate to form fully functional T cells.

Key words: fetal pig, gene expression, immunohistochemistry, thymus

Introduction

Immunohumanized animal models are invaluable tools in research related to human immunity and infection. These models are also useful as animal platforms in preclinical trials in stem-cell-based regenerative medicine, in which damaged tissue can be regenerated *in vivo* by the transplantation of stem cells. Mice models are useful, and immunohumanized mice have been produced by using severely immunodeficient mice such as NOG and NSG mice [5, 7, 14, 22]. However, because of several constraints associated with mouse models, such as small size, short longevity, and a relatively large biological gap with humans, a model using a large animal would be invaluable. In particular, pigs have anatomical and physiological features similar to humans [17], and they have a higher reproductivity rate than other large animals [20]. Thus, pigs make a very attractive model animal. Therefore, we previously developed immunodeficient pigs by targeting the *IL2RG* gene [16] to produce a humanized pig model.

Although an immunohumanized pig model can be theoretically produced using these pigs, some difficulties remain for the efficient reconstitution of the human immune system. For example, the remaining porcine immune system can reject xenogeneic human cells. A severely atrophied thymus in *IL2RG*-knockout pigs [16], which is presumably because of the failure of thymocyte expansion [9], can constrain the development of human T cells. Transplantation to fetal pigs *in utero* can ame-

(Received 26 August 2013 / Accepted 5 December 2013)

Address corresponding: S. Suzuki, Transgenic Pig Research Unit, National Institute of Agrobiological Sciences, 2 Ikenodai, Tsukuba, Ibaraki 305-0901, Japan

liorate these problems because the immunity of the fetus is immature and fetal thymi can normally develop to some extent without the interaction of thymocytes and thymic epithelial cells [9, 19]. However, the differentiation process of fetal porcine thymic function, which plays a significant role in transplantation immunity by generating differentiated T cells, has not been elucidated.

Thymic function has been extensively studied in mice. T-cell progenitors first immigrate from the blood vessels to the cortex of the thymus. This process is at least partially regulated by the chemokine CCL25 and its receptor CCR9 [10, 13]. Thymus-settling cells are subjected to gene rearrangement of the T-cell receptor locus by the recombination-activating gene (*RAG*) complex to become CD4- and CD8-double-positive cells [2, 15]. Double-positive thymocytes which express the T-cell receptor complex having a low avidity with the self-peptide presented by the major histocompatibility complex (MHC) on the surface of cortical epithelial cells are selected to survive. The unique population of peptides that are generated by thymic-specific proteasomes (β5t) which are expressed exclusively in thymic cortical epithelial cells deeply commits to this process by interacting with MHC class I [21]. The positively selected thymocytes migrate to the medulla by CCL19 and CCR7 signals [18]. Then, the thymocytes that interact with the self-antigen presented by medullary epithelial cells or dendritic cells with a high avidity are eliminated by apoptosis [15]. This process, which is called negative selection, is at least partially dependent on the autoimmune regulator (Aire), which has been suggested to be a regulator of the expression of the peripheral self-antigen [1] or the differentiation of medullary epithelial cells [4, 23]. Thymocytes that escape negative selection finally emigrate out of the thymus as CD4- or CD8-single-positive cells.

In this study, we examined the levels of gene expression of several marker proteins and factors considered to be relevant to thymic function, together with a histological analysis, to examine the developmental stage of each fetal thymus. In addition, we also intended to further elucidate porcine thymic function by examining the fetal thymi sequentially, which was otherwise very difficult because all the thymic processes simultaneously occur in the postnatal thymi.

Materials and Methods

Experimental animals

The animals that were used in this study were healthy cross-bred pigs (*Sus scrofa*) that were conventionally reared in the National Institute of Livestock and Grassland Sciences. All animal experiments were approved by the Animal Care Committee of the National Institute of Agrobiological Sciences.

Collection of tissues from fetal and newborn pigs

At 35, 40, 45, 50, 55, 65, and 85 days of gestation (DG), two pregnant female pigs for each stage were sacrificed, and their fetuses were recovered. In addition, newborn piglets were sacrificed at 2 days postpartum (DP). From these fetuses or piglets, thymi were collected for quantitative RT-PCR and immunohistochemistry. In the case of fetuses at DG35–DG50, the entire cervical portions of the fetus were excised for the histological analysis.

Total RNA extraction and RT-PCR

Total RNA was extracted with Sepazol (Nakalai Tesque, Inc., Kyoto, Japan) according to the manufacturer's instructions. After being treated with DNase I (TaKaRa Bio Inc., Otsu, Japan) at 37°C for 30 min, RNA was subjected to first-strand cDNA synthesis at 37°C for 30 min with a PrimeScript RT reagent kit (TaKaRa Bio Inc.).

Real-time quantitative RT-PCR of the transcripts of interest was performed with a LightCycler instrument (Roche Diagnostics, Basel, Switzerland). PCR amplification was performed in a 20-μl reaction mixture consisting of 1 μl of cDNA, 0.4 μM of each primer, and 10 μl of SYBR premix Ex Taq II (TaKaRa Bio Inc.). The cycling conditions were 95°C for 3 min, which was followed by 60 cycles at 95°C for 5 sec, 55°C or 58°C for 30 sec each, and 72°C for 30 sec. The primers that were used are indicated in Table 1. The relative quantification of target gene expression was normalized against the expression of the hypoxanthine phosphoribosyltransferase 1 (*HPRT1*) gene.

Immunohistochemistry

Thymi or slices of cervical portions were embedded in molds with OCT compound, snap frozen in liquid nitrogen, and then stored at −80°C. Frozen tissues were sectioned at 6 μm with a cryostat (HM-500; Carl Zeiss

Table 1. The sequences of the primers that were used in quantitative RT-PCR

	forward	reverse	accession No.
FOXN1	TGACGGAGCACTTTCCTTAC	TGCATCTTGTCGATCTTGGC	DB803240
PSMB11	GCTACGACATGAGCACCCAG	ACTCTCCCGCACGTGGAAGA	XM_001925763
AIRE	ATGTCCACTTCGGTCCAGAG	CCTGGATGCACTTCTTGGAG	XM_003358989
CCL25	TCCTGCTATCCATGCTCAAG	ATATCACAGCAGGCAGGTTG	NM_001025214
CCR9	CAGAAGCCGCAAGTCTGATG	AACACGAGCCAGTACAATGG	NM_001001624
CCL19	GCTAAGCCTCTGGACTTCTC	CAGCCATCTCGAATGAGCAG	NM_001170516
CCR7	TGAAGAAGAGCCTGCTGGTG	TAAAGGTCCGCACGTCCTTC	NM_001001532
PTPRC	ACAAGGTGGATGTCTATGGC	CAAGCTCACTTCTGTTTCTC	XM_003130596
IL2RG	CTTGGAACAGCAGCTCTGAG	ACCAACAGCCAGAAGTGATC	NM_214083
CD3E	GTAGTTGACATCTGCATCAC	TGGGCTCATAGTCTGGATTG	NM_214227
RAG1	ATGCGGAGAAGGTCCTTCTG	CACTGGGTAATCGTCCACAG	NM_001123184
RAG2	TCTCATGGAGATGGGCATTG	CTTGCTATCTCCACATGCTC	NM_001128481
FOXP3	CATGGAGTACTTCAAGTTCC	AACATGCGTGTGAACCAGTG	NM_001128438
HPRT1	TACTGTAATGACCAGTCAACG	GCAACCTTGACCATCTTTGG	NM_001032376

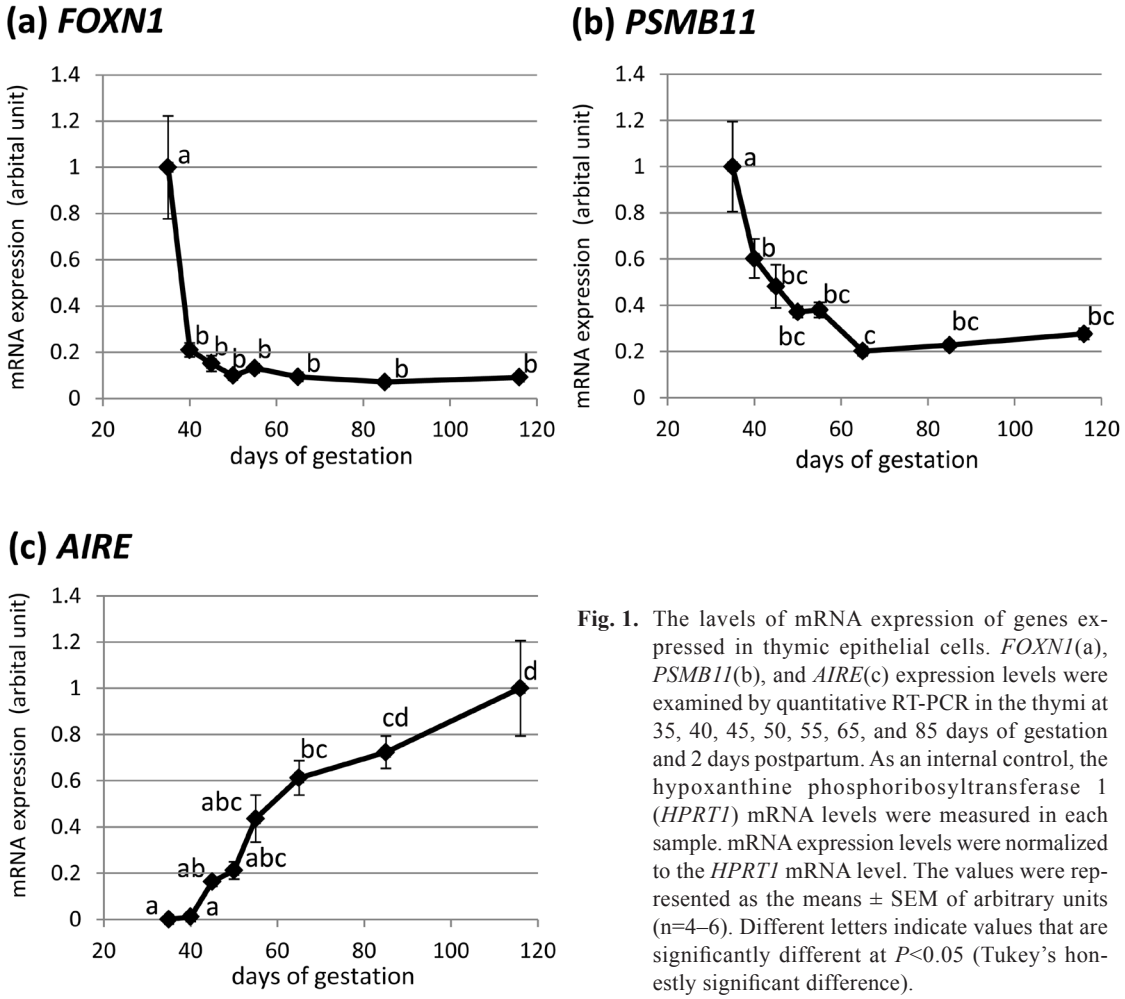

Fig. 1. The lavels of mRNA expression of genes expressed in thymic epithelial cells. *FOXN1*(a), *PSMB11*(b), and *AIRE*(c) expression levels were examined by quantitative RT-PCR in the thymi at 35, 40, 45, 50, 55, 65, and 85 days of gestation and 2 days postpartum. As an internal control, the hypoxanthine phosphoribosyltransferase 1 (*HPRT1*) mRNA levels were measured in each sample. mRNA expression levels were normalized to the *HPRT1* mRNA level. The values were represented as the means ± SEM of arbitrary units (n=4–6). Different letters indicate values that are significantly different at $P<0.05$ (Tukey's honestly significant difference).

Microscopy GmbH, Jena, Germany). Cryosections were air dried at room temperature and fixed with 4% paraformaldehyde in phosphate-buffered saline [PBS (−)] for 15 min. After washing with PBS (−), antigen retrieval was performed in a food steamer (Twinbird Corporation, Tsubame, Japan) with 10-mM citrate buffer

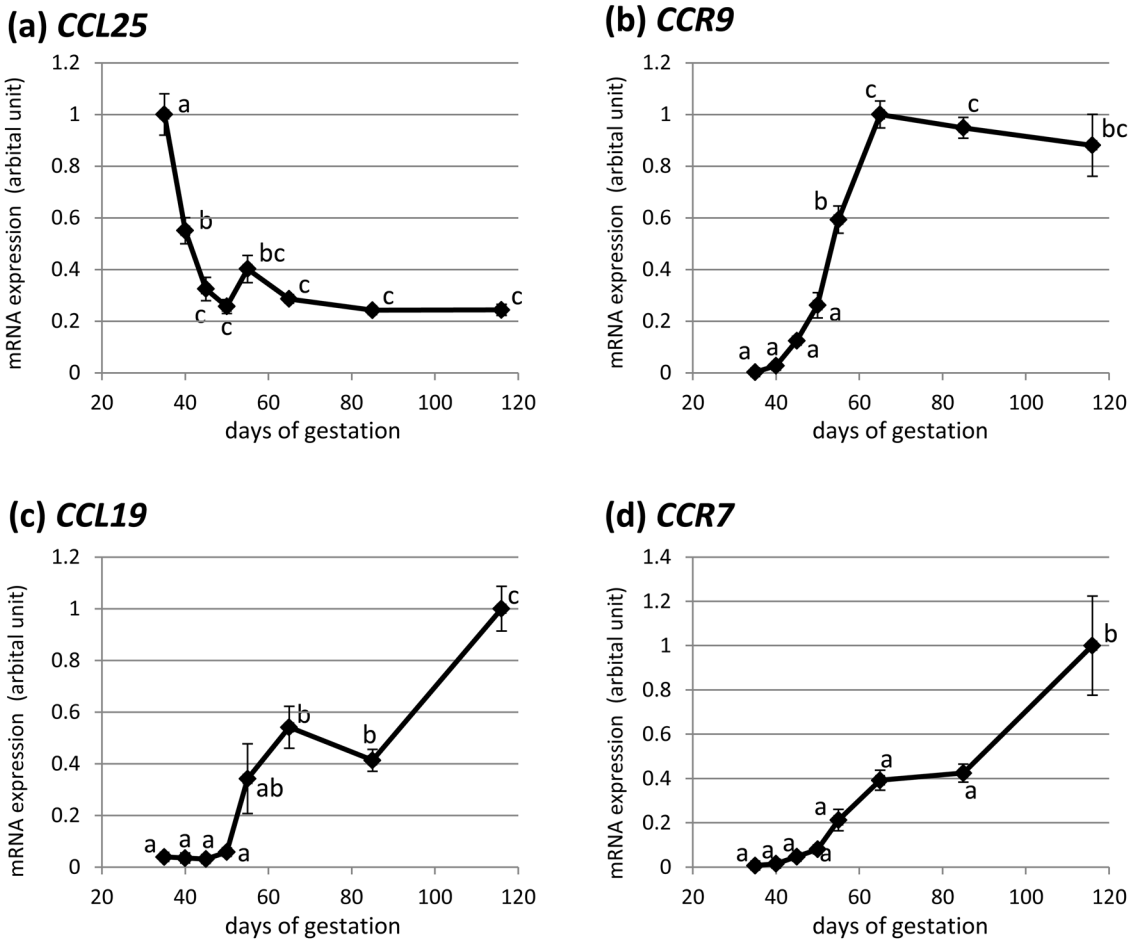

Fig. 2. The levels of mRNA expression of genes that are involved in the migration of thymocytes. *CCL25* (a), *CCR9* (b), *CCL19* (c), and *CCR7* (d) expression levels were examined by quantitative RT-PCR in the thymi at 35, 40, 45, 50, 55, 65, and 85 days of gestation and 2 days postpartum. As an internal control, the hypoxanthine phosphoribosyltransferase 1 (*HPRT1*) mRNA levels were measured in each sample. mRNA expression levels were normalized to the *HPRT1* mRNA levels. The values are represented as the means ± SEM of arbitrary units (n=4–6). Different letters indicate values that are significantly different at $P<0.05$ (Tukey's honestly significant difference).

(pH 6.0) for 25 min. The sections were washed with PBS (−) and incubated in 10% normal rabbit serum (for Foxn1, with 0.05% Tween20) or 10% normal goat serum (for CK5) for 60 min at room temperature to decrease nonspecific staining. The sections were then incubated overnight at 4°C with a primary antibody against FOXN1 [Abcam Plc, Cambridge, UK ; 1:50 dilution in PBS (−), 1% bovine serum albumin (BSA), and 0.05% Tween20], AIRE [Everest Biotech Ltd.., Oxfordshire, UK ; 1:750 in PBS (−) and 1% BSA], or CK5 [Abcam plc; 1:100 in PBS (−) and 1% BSA]. After washing with PBS (−), they were treated with 0.3% H_2O_2 in PBS (−) for 15 min to quench endogenous peroxidase activity. After washing with PBS (−), sections were incubated with anti-goat IgG horseradish peroxidase-coupled polymer ImmPRESS (Vector Laboratories, Inc., Burlingame, CA, USA) for 30 min (for FOXN1 and AIRE) or horseradish peroxidase-conjugated anti-rabbit IgG (Bethyl Laboratories, Inc., Montgomery, TX, USA ; 1:100 in PBS (−) and 1% BSA) for 60 min (for CK5), and this was followed by detection with 3,3′-diaminobenzidine [Peroxidase Stain DAB Kit (Brown Stain); Nacalai Tesque, Inc.]. Then, the sections were lightly counterstained with Mayer's hematoxylin (2 min), dehydrated, and mounted with Entellan™ new (Merck Millipore, Darmstadt, Germany).

Statistical analysis

Statistical analyses were performed using Tukey's

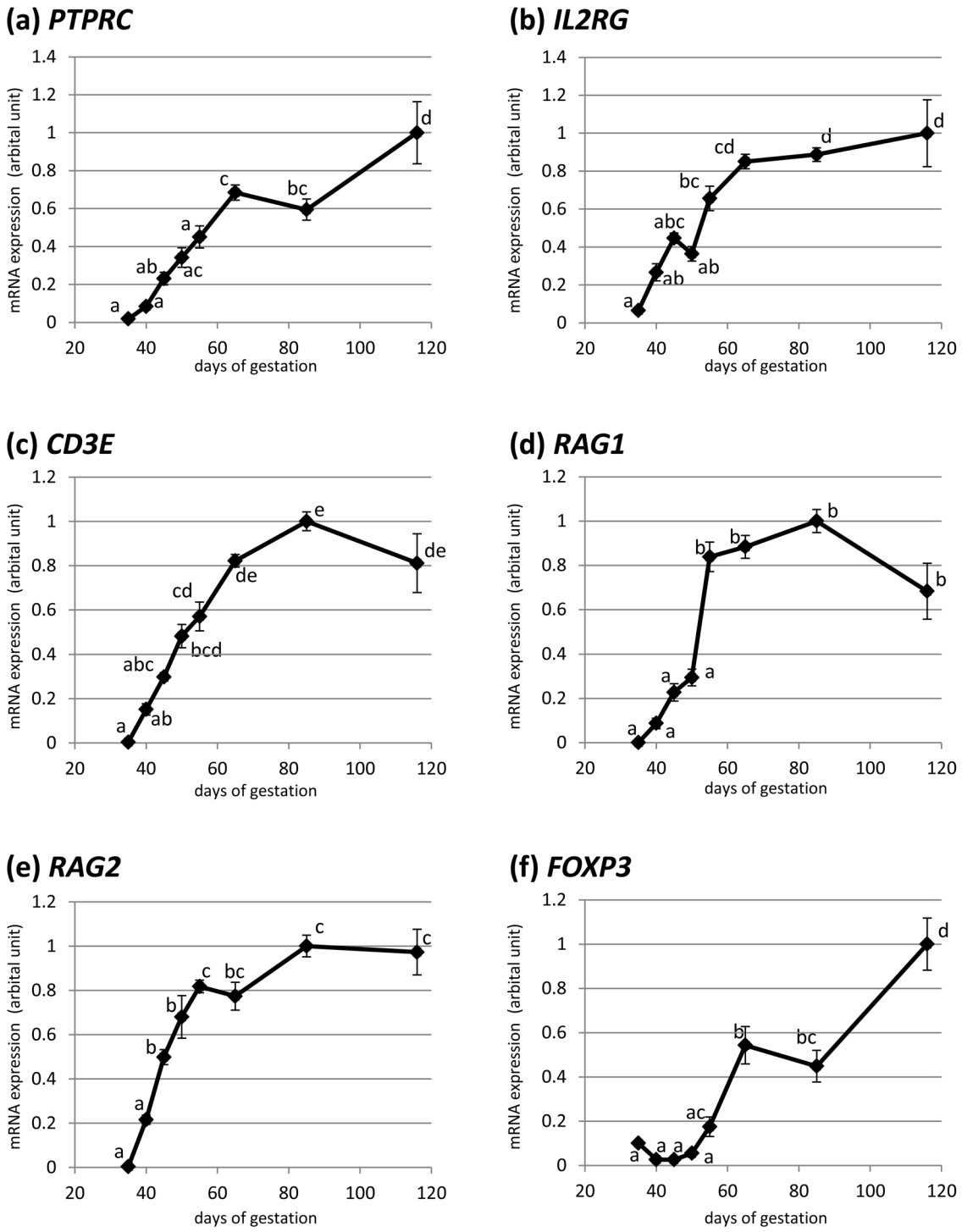

Fig. 3. The levels of mRNA expression of genes expressed in thymocytes. *PTPRC*(a), *IL2RG*(b), *CD3E*(c), *RAG1*(d), *RAG2*(e), and *FOXP3*(f) expression levels were examined by quantitative RT-PCR in the thymi at 35, 40, 45, 50, 55, 65, and 85 days of gestation and 2 days postpartum. As an internal control, the hypoxanthine phosphoribosyltransferase 1 (*HPRT1*) mRNA levels were measured in each sample. mRNA expression levels were normalized to the *HPRT1* mRNA levels. The values are represented as the means ± SEM of arbitrary units (n=4–6). Different letters indicate values that are significantly different at $P<0.05$ (Tukey's honestly significant difference).

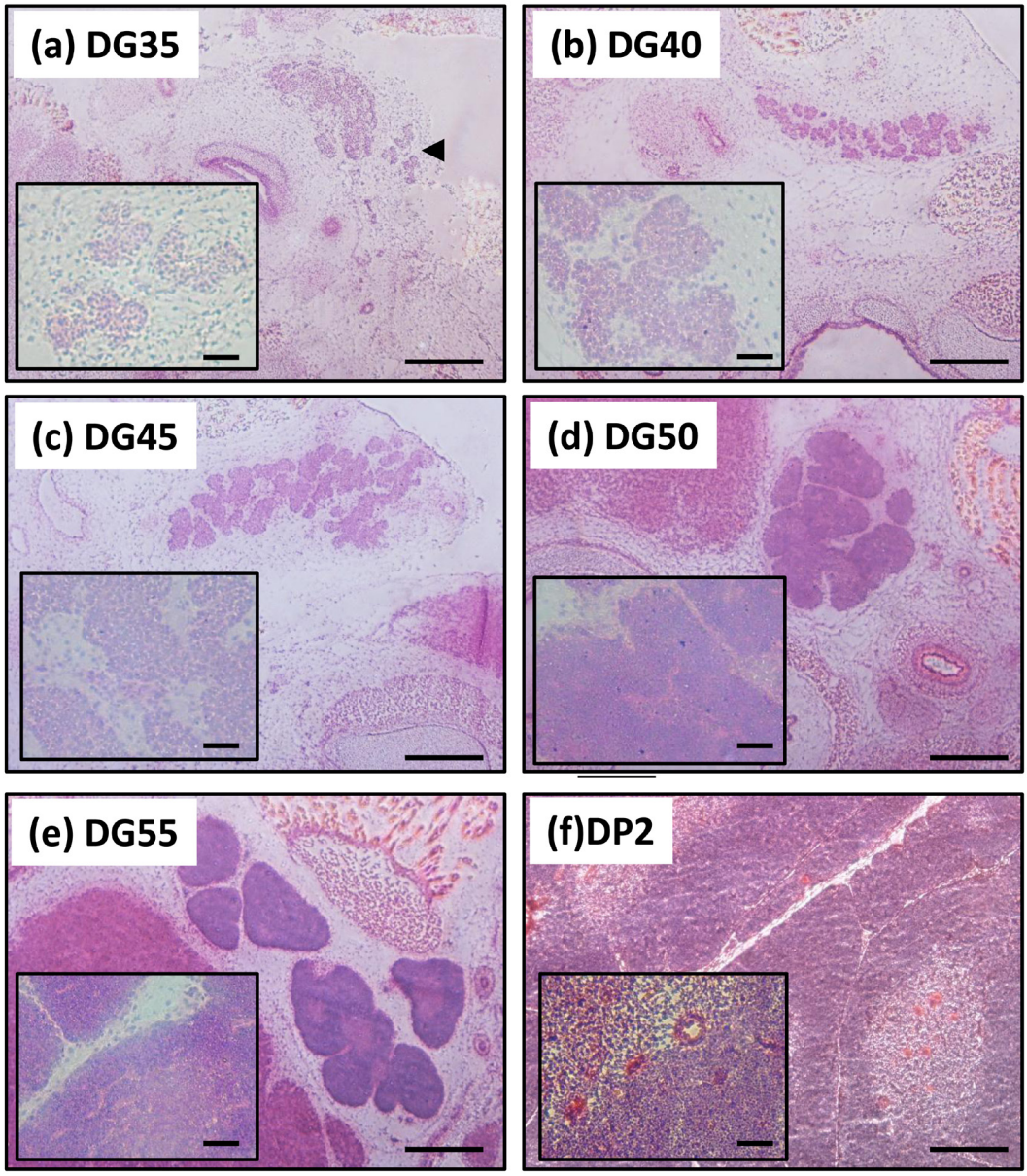

Fig. 4. Histological examination of the development of porcine fetal thymi. The thymi at 35 (a), 40 (b), 45 (c), 50 (d), and 55 (e) days of gestation and at 2 days postpartum (f) were subjected to hematoxylin and eosin staining. The arrowhead in (a) points to the area of the thymus. The scale bars represent 500 μm. The inserts show images with a higher magnification (Scale bars=100 μm).

Honestly Significant Differences test (HSD). *P* values less than 0.05 were considered statistically significant.

Results and Discussion

To outline the developmental process of thymi, we first examined the expression patterns of several genes that are expressed in thymic epithelial cells and thymocytes. The relative expression levels of *FOXN1* a key regulator for the thymic organogenesis and *PSMB11*, which encodes the thymic proteasome β5t in whole thymi, were highest at DG35, and they declined with fetal development (Figs. 1a and 1b). This suggested that the thymic cortical epithelial cells were differentiated at DG35, and the subsequent decline in the relative expression levels reflected a decrease in the relative abundance

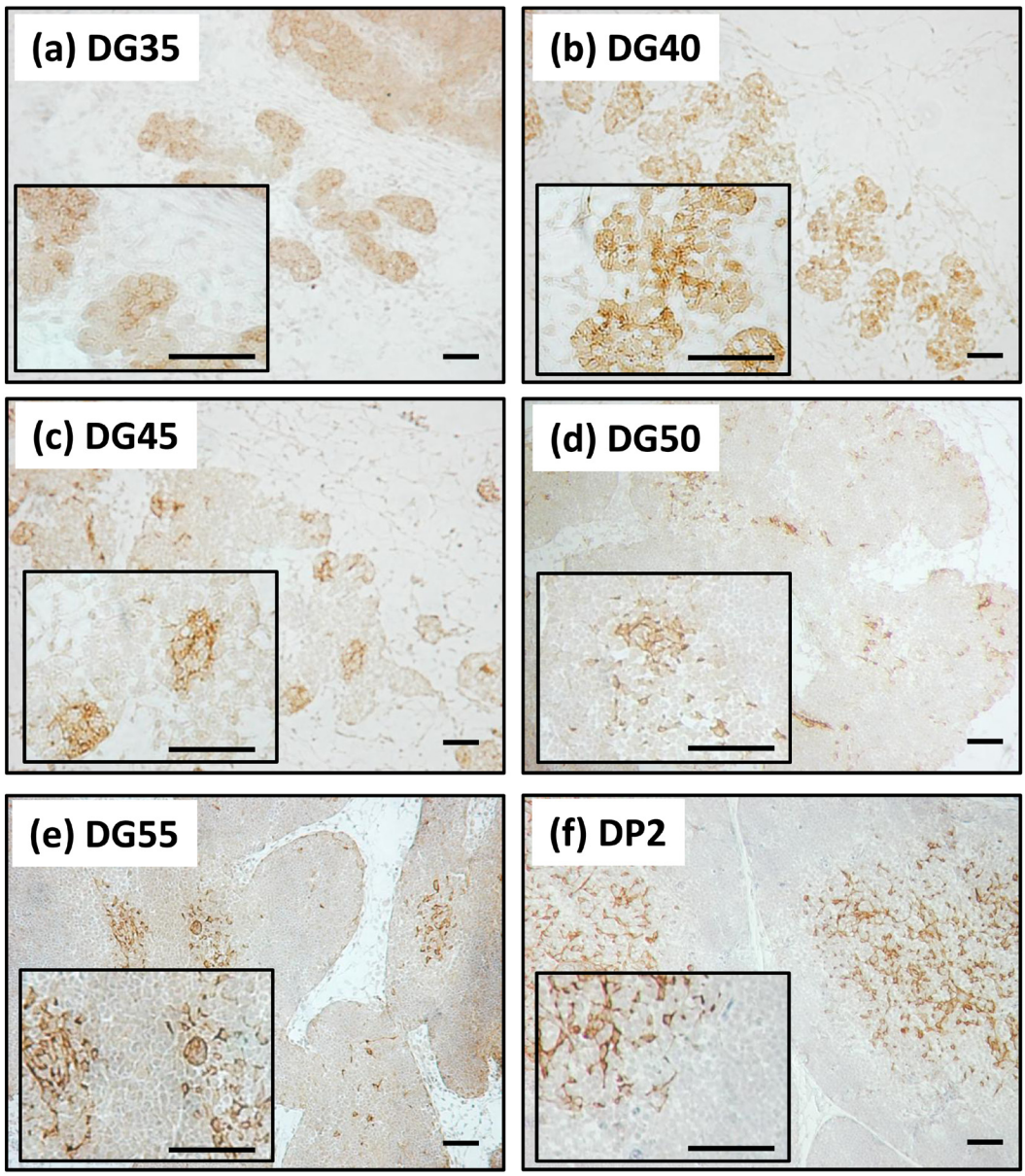

Fig. 5. Immunohistochemical analysis of cytokeratin 5 in porcine fetal thymi. The thymi at 35 (a), 40 (b), 45 (c), 50 (d), and 55 (e) days of gestation and at 2 days postpartum (f) were stained with an anti-CK5 antibody. The scale bars represent 100 μm. The inserts show images with a higher magnification (Scale bars=50 μm).

of thymic cortical epithelial cells within the thymi because of an increase in other types of cells with thymic development. The levels of *AIRE*, which is expressed in medullary thymic epithelial cells [6], increased from DG45 to DP2 (Fig. 1c). This suggested that the thymic medulla began to develop around at DG45 and that the development continued throughout the fetal stage.

Next, we examined the expression pattern of genes that affect the migration of thymocytes. *CCL25*, which is a chemokine, plays a significant role in the recruitment of T-cell progenitors to the thymus. *CCL25* was highly expressed as early as DG35 (Fig. 2a). The expression of *CCR9*, which is widely expressed in thymus-settling T-cell progenitors, rapidly increased from DG40 to DG65 (Fig. 2b). This reflected the vigorous settlement and/or expansion of T-cell progenitors in thymi during this period. The levels of expression of *CCL19* and *CCR7*, which are related to the cortex–medulla migration

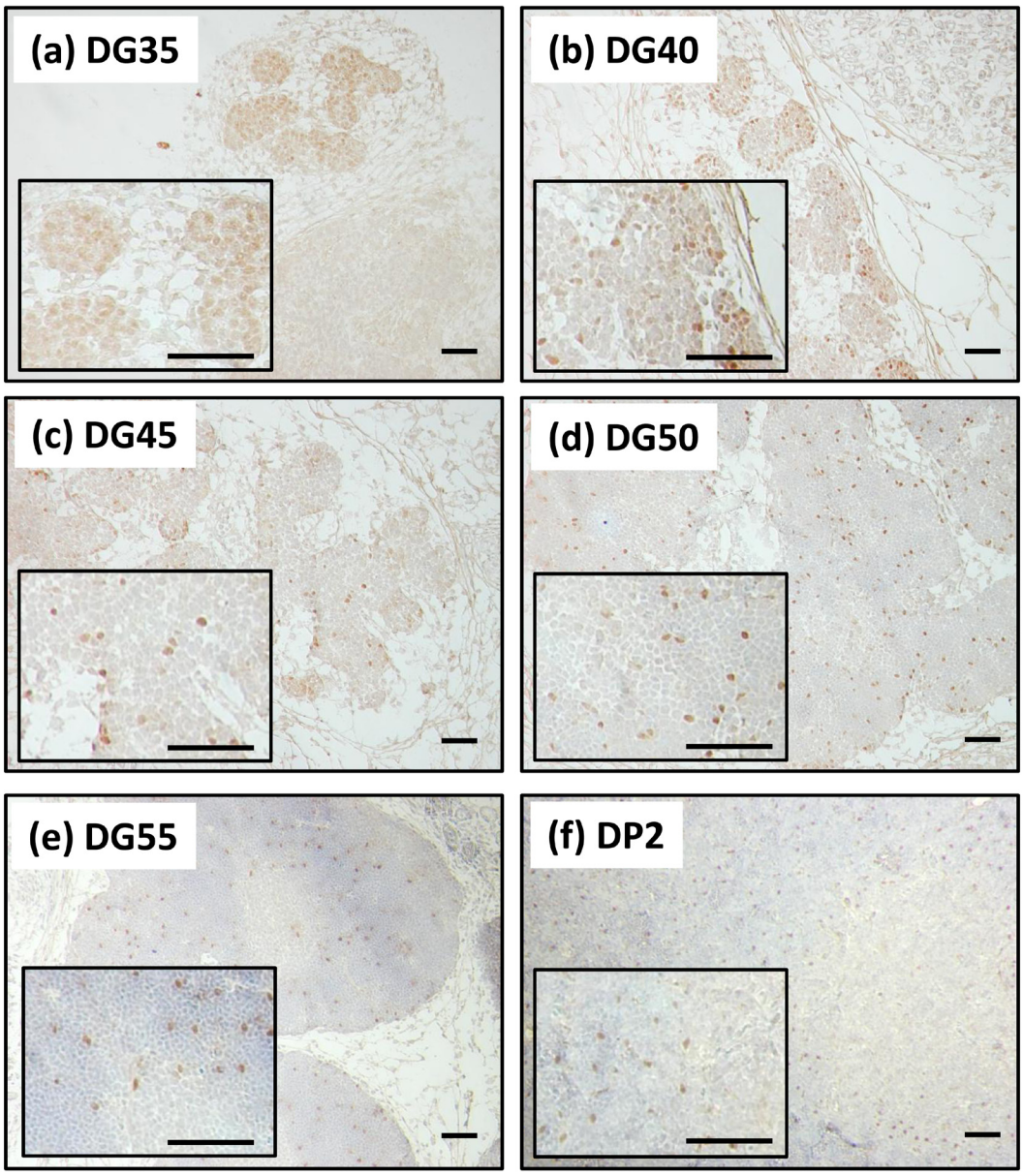

Fig. 6. Immunohistochemical analysis of FOXN1 in porcine fetal thymi. The thymi at 35 (a), 40 (b), 45 (c), 50 (d), and 55 (e) days of gestation and at 2 days postpartum (f) were stained with an anti-FOXN1 antibody. The scale bars represent 100 μm. The inserts show images with a higher magnification (Scale bars=50 μm).

of thymocytes, were also examined. *CCR7* expression began to increase at DG50–DG55, and *CCL19* expression began to increase simultaneously (Figs. 2c and 2d). These results might suggest that the positive selection process, which makes thymocytes *CCR7* positive, began to be manifested from approximately DG50 and that the cortex–medulla migration was immediately activated by DG55 when the medulla had developed to some extent, as expected from the expression pattern of *AIRE*.

The levels of expression of *PTPRC*, which encodes the hematopoietic markers CD45 and *IL2RG*, widely expressed in immune cells, showed a similar increasing pattern in the entire phase of analysis (Fig. 3a and 3b), which was considered to be a reflection of the continuous inflow to and the settlement of T-cell progenitors in thymi. In addition, the expressions of *CD3E*, which encodes the essential component of the T-cell receptor, and *RAG1* and *RAG2*, which are indispensable factors for

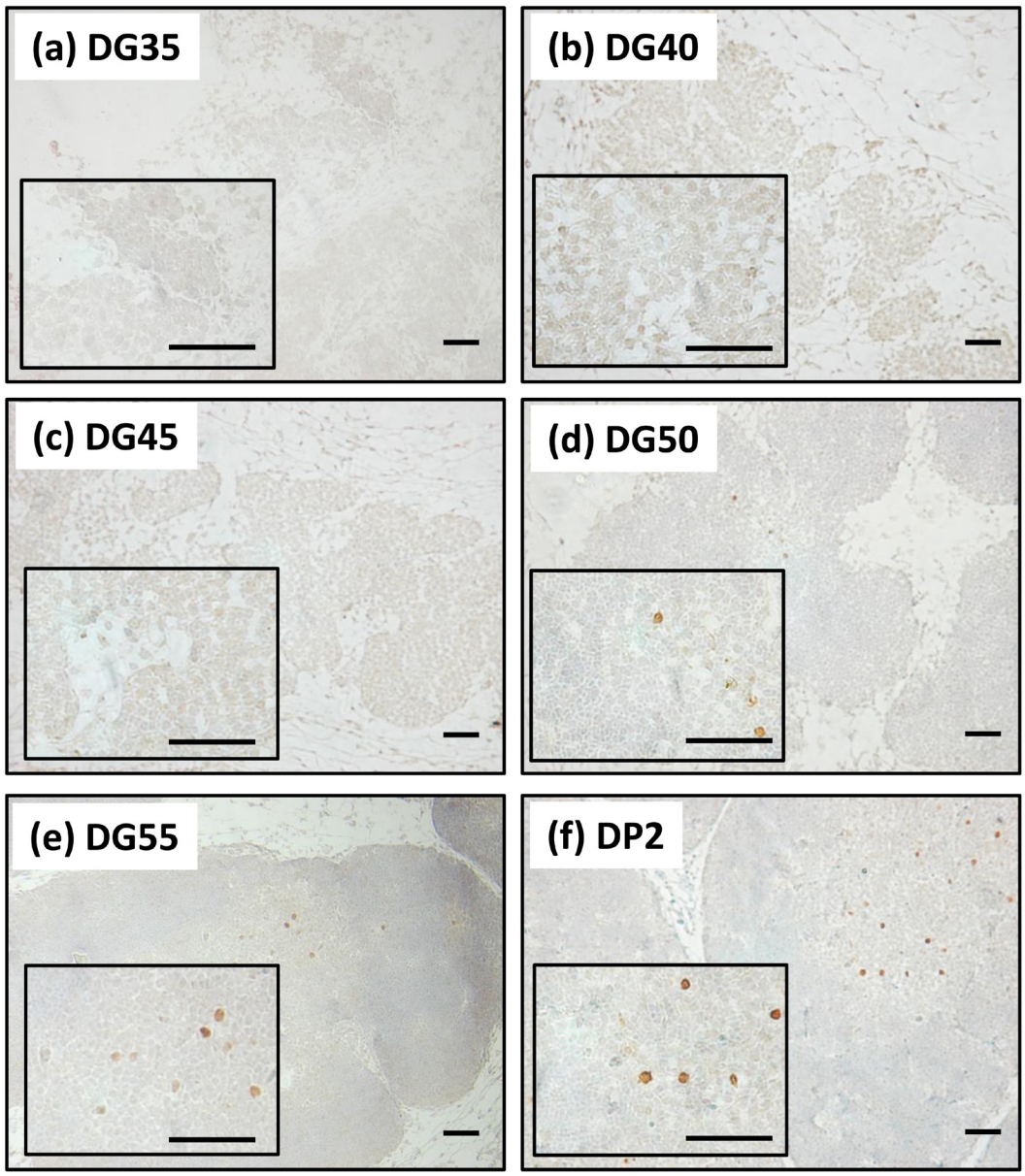

Fig. 7. Immunohistochemical analysis of AIRE in porcine fetal thymi. The thymi at 35 (a), 40 (b), 45 (c), 50 (d), and 55 (e) days of gestation and at 2 days postpartum (f) were stained with an anti-AIRE antibody. The scale bars represent 100 μm. The inserts show images with a higher magnification (Scale bars=50 μm).

the rearrangement of T-cell receptor genes, rapidly increased from DG40 to DG65 (Figs. 3c, 3d, and 3e). These findings might suggest that T-cell progenitors that settled in thymi were immediately subjected to the differentiation process in the thymic cortex prior to the formation of the thymic medulla. However, the expression of *FOXP3*, which is the factor that is critical for the differentiation of regulatory T cells, began to increase at DG55 (Fig. 3f), which suggested that their differentiation depended on the medulla.

To outline the developmental process of thymi, we first performed hematoxylin and eosin (H&E) staining on the sections of the cervical portion of porcine fetuses at DG35, DG40, DG45, DG50, and DG55, as well as on the thymic section of newborn piglets (Fig. 4). The well-developed thymi of newborn piglets had two distinct areas: a darker-staining cortex and a lighter-staining medulla that was surrounded by the cortex. The darker

staining by hematoxylin was considered to correspond to the dense accumulation of thymocytes. At DG35, the lobular structure that is characteristic of the thymus was already formed, but it was still loosely organized. As the fetuses developed, the thymic lobes gradually became tightly organized, and no light-staining medulla could be observed until DG45. At DG50, some medulla-like areas were faintly observed in the inner region. A distinct medulla was observed at DG55.

To detect the medulla formation more clearly, we performed an immunohistochemical analysis with cytokeratin 5 (CK5), which is a marker protein for the thymic medulla [8] (Fig. 5). We first confirmed that the staining pattern for CK5 was restricted to the thymic medulla with the areas that were lightly stained with hematoxylin in the thymic sections of the newborn pig. At DG35 and DG40, CK5 staining was detected in a scattered pattern throughout the thymic lobes, suggesting that CK5 is expressed in the cortical epithelium before the formation of a distinct cortex–medulla organization. From DG45 to DG50, CK5 staining was gradually localized to the inner region of the thymic lobes, which showed that the medulla formation began in this stage. At DG55, distinct CK5 staining was detected in the inner region of the thymic lobe, and this corresponded to the lightly stained area. This result, together with the abovementioned observations of H&E staining, suggested that cortex–medulla organization begins from DG45 to DG50 and that it was apparently clarified up to DG55.

In addition, the localization of characteristic transcription factors of thymic epithelial cells was examined by immunohistochemistry. FOXN1 is an invaluable factor for both cortical and medulla epithelial cells, and it has been reported to be expressed in both types of epithelial cells, including immature cells, in mice [3, 11, 12]. At DG35, almost all cells expressed FOXN1 protein, and this corresponded to the differentiation of the thymic epithelial cells (Fig. 6a), although the expression levels of each cell appeared to be lower than those at later stages. This difference may reflect the distinct developmental status of thymic epithelial cells at each fetal stage. FOXN1-positive cells in the thymi were detected in a scattered pattern in all stages examined (Fig. 6), although the frequency of positive cells was decreased, especially from DG40 to DG45. This decrease can be attributed to the inflow and expansion of T-cell progenitors, which eventually become the dominant population in the thymus, as expected by the expression of *PTPRC*. AIRE is considered to be a key factor in the differentiation and/or function of medullary epithelial cells, and its expression is essentially restricted to these cells [6]. Similarly, we detected a medulla-restricted expression of AIRE after DG50 synchronously with the medulla formation that was characterized by CK5 expression (Fig. 7).

Collectively, porcine thymic function might be considered to be roughly completed around DG50 to DG55, as determined by the formation of the thymic medulla. Therefore, it is possible that the circulating T cells after DG50 have been selected to survive by the positive and negative selection in thymi and can be functional in immune rejection. However, we inevitably need to precisely unravel the activities of the innate, humoral and cellular immunity in porcine fetuses to determine the optimal window for the transplantation of xenogeneic human cells.

Moreover, our gene expression analyses suggested that genes that are critically involved in thymic functions in mice are also significant in the porcine thymus. It was also suggested that the stepwise developmental processes of porcine thymic epithelial cells and thymocytes may be essentially similar to those in mice. Overall, this study provided pioneering information for the further elucidation of porcine thymic function.

Acknowledgment

The authors would like to thank the staff of the Swine Management Section of the National Institute of Livestock and Grassland Science for taking care of the pigs, and N. Watanabe and K. Iijima for technical assistance.

Refernces

1. Anderson, M.S., Venanzi, E.S., Klein, L., Chen, Z., Berzins, S.P., Turley, S.J., von Boehmer, H., Bronson, R., Dierich, A., Benoist, C., and Mathis, D. 2002. Projection of an immunological self shadow within the thymus by the aire protein. *Science* 298: 1395–1401. [Medline] [CrossRef]
2. Bassing, C.H., Swat, W., and Alt, F.W. 2002. The mechanism and regulation of chromosomal V(D)J recombination. *Cell* 109: S45–S55. [Medline] [CrossRef]
3. Bleul, C.C., Corbeaux, T., Reuter, A., Fisch, P., Mönting, J.S., and Boehm, T. 2006. Formation of a functional thymus initiated by a postnatal epithelial progenitor cell. *Nature* 441: 992–996. [Medline] [CrossRef]
4. Dooley, J., Erickson, M., and Farr, A.G. 2008. Alterations of the medullary epithelial compartment in the Aire-deficient

thymus: implications for programs of thymic epithelial differentiation. *J. Immunol.* 181: 5225–5232. [Medline]

5. Hiramatsu, H., Nishikomori, R., Heike, T., Ito, M., Kobayashi, K., Katamura, K., and Nakahata, T. 2003. Complete reconstitution of human lymphocytes from cord blood CD34+ cells using the NOD/SCID/gammacnull mice model. *Blood* 102: 873–880. [Medline] [CrossRef]
6. Hubert, F.X., Kinkel, S.A., Webster, K.E., Cannon, P., Crewther, P.E., Proeitto, A.I., Wu, L., Heath, W.R., and Scott, H.S. 2008. A specific anti-Aire antibody reveals aire expression is restricted to medullary thymic epithelial cells and not expressed in periphery. *J. Immunol.* 180: 3824–3832. [Medline]
7. Ishikawa, F., Yasukawa, M., Lyons, B., Yoshida, S., Miyamoto, T., Yoshimoto, G., Watanabe, T., Akashi, K., Shultz, L.D., and Harada, M. 2005. Development of functional human blood and immune systems in NOD/SCID/IL2 receptor γ chain(^{null}) mice. *Blood* 106: 1565–1573. [Medline] [CrossRef]
8. Klug, D.B., Carter, C., Crouch, E., Roop, D., Conti, C.J., and Richie, E.R. 1998. Interdependence of cortical thymic epithelial cell differentiation and T-lineage commitment. *Proc. Natl. Acad. Sci. USA* 95: 11822–11827. [Medline] [CrossRef]
9. Klug, D.B., Carter, C., Gimenez-Conti, I.B., and Richie, E.R. 2002. Cutting edge: thymocyte-independent and thymocyte-dependent phases of epithelial patterning in the fetal thymus. *J. Immunol.* 169: 2842–2845. [Medline]
10. Lai, A.Y. and Kondo, M. 2007. Identification of a bone marrow precursor of the earliest thymocytes in adult mouse. *Proc. Natl. Acad. Sci. USA* 104: 6311–6316. [Medline] [CrossRef]
11. Nehls, M., Kyewski, B., Messerle, M., Waldschütz, R., Schüddekopf, K., Smith, A.J., and Boehm, T. 1996. Two genetically separable steps in the differentiation of thymic epithelium. *Science* 272: 886–889. [Medline] [CrossRef]
12. Rossi, S.W., Jenkinson, W.E., Anderson, G., and Jenkinson, E.J. 2006. Clonal analysis reveals a common progenitor for thymic cortical and medullary epithelium. *Nature* 441: 988–991. [Medline] [CrossRef]
13. Schwarz, B.A., Sambandam, A., Maillard, I., Harman, B.C., Love, P.E., and Bhandoola, A. 2007. Selective thymus settling regulated by cytokine and chemokine receptors. *J. Immunol.* 178: 2008–2017. [Medline]
14. Shultz, L.D., Lyons, B.L., Burzenski, L.M., Gott, B., Chen, X., Chaleff, S., Kotb, M., Gillies, S.D., King, M., Mangada, J., Greiner, D.L., and Handgretinger, R. 2005. Human lymphoid and myeloid cell development in NOD/LtSz-scid IL2R gamma null mice engrafted with mobilized human hemopoietic stem cells. *J. Immunol.* 174: 6477–6489. [Medline]
15. Starr, T.K., Jameson, S.C., and Hogquist, K.A. 2003. Positive and negative selection of T cells. *Annu. Rev. Immunol.* 21: 139–176. [Medline] [CrossRef]
16. Suzuki, S., Iwamoto, M., Saito, Y., Fuchimoto, D., Sembon, S., Suzuki, M., Mikawa, S., Hashimoto, M., Aoki, Y., Najima, Y., Takagi, S., Suzuki, N., Suzuki, E., Kubo, M., Mimuro, J., Kashiwakura, Y., Madoiwa, S., Sakata, Y., Perry, A.C., Ishikawa, F., and Onishi, A. 2012. Il2rg gene-targeted severe combined immunodeficiency pigs. *Cell Stem. Cell* 10: 753–758. [Medline] [CrossRef]
17. Swindle, M. and Smith, A. 1998. Comparative anatomy and physiology of the pig. *Scand. J. Lab. Anim. Sci.* 25: 11–21.
18. Ueno, T., Saito, F., Gray, D.H., Kuse, S., Hieshima, K., Nakano, H., Kakiuchi, T., Lipp, M., Boyd, R.L., and Takahama, Y. 2004. CCR7 signals are essential for cortex-medulla migration of developing thymocytes. *J. Exp. Med.* 200: 493–505. [Medline] [CrossRef]
19. van Ewijk, W., Holländer, G., Terhorst, C., and Wang, B. 2000. Stepwise development of thymic microenvironments in vivo is regulated by thymocyte subsets. *Development* 127: 1583–1591. [Medline]
20. Wolf, E., Schernthaner, W., Zakhartchenko, V., Prelle, K., Stojkovic, M., and Brem, G. 2000. Transgenic technology in farm animals—progress and perspectives. *Exp. Physiol.* 85: 615–625. [Medline] [CrossRef]
21. Xing, Y., Jameson, S.C., and Hogquist, K.A. 2013. Thymoproteasome subunit-β5T generates peptide-MHC complexes specialized for positive selection. *Proc. Natl. Acad. Sci. USA* 110: 6979–6984. [Medline] [CrossRef]
22. Yahata, T., Ando, K., Nakamura, Y., Ueyama, Y., Shimamura, K., Tamaoki, N., Kato, S., and Hotta, T. 2002. Functional human T lymphocyte development from cord blood CD34+ cells in nonobese diabetic/Shi-scid, IL-2 receptor gamma null mice. *J. Immunol.* 169: 204–209. [Medline]
23. Yano, M., Kuroda, N., Han, H., Meguro-Horike, M., Nishikawa, Y., Kiyonari, H., Maemura, K., Yanagawa, Y., Obata, K., Takahashi, S., Ikawa, T., Satoh, R., Kawamoto, H., Mouri, Y., and Matsumoto, M. 2008. Aire controls the differentiation program of thymic epithelial cells in the medulla for the establishment of self-tolerance. *J. Exp. Med.* 205: 2827–2838. [Medline] [CrossRef]